

Double sneutrino in ation and its phenom enologies

Xiao-Jun Bi, Bo Feng,^y and Xinmin Zhang^z

Institute of High Energy Physics, Chinese Academy of Sciences,

P.O. Box 918-4, Beijing 100039, People's Republic of China

(Dated: March 24, 2024)

Abstract

In this paper we study double scalar neutrino in ation in the minimal supersymmetric seesaw model in light of WMAP. In ation in this model is firstly driven by the heavier sneutrino field N_2 and then the lighter field N_1 . We will show that with the mass ratio $6 < M_2/M_1 < 10$ the model predicts a suppressed primordial scalar spectrum around the largest scales and the predicted CMB TT quadrupole is much better suppressed than the single sneutrino model. So this model is more favored than the single sneutrino in ation model. We then consider the implications of the model on the reheating temperature, leptogenesis and lepton flavor violation. Our results show that the seesaw parameters are constrained strongly by the reheating temperature, together with the requirement by a successful in ation. The mixing between the first generation and the other two generations in the right-handed neutrino sector is tiny. The rates of lepton flavor violating processes in our scenario depend on only 4 unknown seesaw parameters through a 'reduced' seesaw formula, besides U_{e3} and the supersymmetric parameters. We find that the branching ratio of $\tau \rightarrow e \gamma$ is generally near the present experimental limit, while $\text{Br}(\tau \rightarrow \mu \gamma)$ is around $O(10^{10} - 10^9)$.

Em ail: bjxj@mail.ihep.ac.cn

^yEm ail: fengbo@mail.ihep.ac.cn

^zEm ail: xmzhang@mail.ihep.ac.cn

I. INTRODUCTION

It is widely accepted today that the early universe has experienced an era of accelerated expansion known as inflation [1]. Inflationary universe has solved many problems of the standard hot big-bang cosmology, such as the flatness and horizon problems. In addition, it provides a causal interpretation for the origin of the density fluctuations in the Cosmic Microwave Background (CMB) and large scale structure (LSS).

Among current inflation models, sneutrino chaotic inflation [2, 3] is one of the promising physical candidates where inflation is driven by the superpartner of the right-handed (RH) neutrino. In this scenario, no extra inflation scalar field is needed, besides the RH sneutrinos, which are necessary to explain the tiny neutrino mass [4] in the minimal supersymmetric seesaw mechanism [5]. Baryon number asymmetry via leptogenesis [6] can also be easily realized in this framework.

The single sneutrino inflation model predicts a near scale invariant primordial power spectrum. Despite the fact that the scale invariant primordial spectrum is consistent with current Wilkinson Microwave Anisotropy Probe (WMAP) observations [7], it is noted that there might be possible discrepancies between predictions and observations on the largest and smallest scales. WMAP data show a low TT quadrupole [8] as previously detected by COBE [9]. In Ref. [10] Peiris et al. find that WMAP data alone favor a large running of the spectral index from blue to red at > 1.5 with $dn_s = d \ln k = 0.077^{+0.050}_{-0.052}$. When adding LSS data of 2DFGRS [11] the running is more favored with $dn_s = d \ln k = 0.075^{+0.044}_{-0.045}$.

The most proper way to get the shape of the spectrum from observations should be the primordial spectrum reconstruction [12, 13, 14]. A detailed reconstruction of the power spectrum by Mukherjee and Wang [12] shows that a running of the index is favored. Ref. [13] reconstructs the primordial spectrum with WMAP data and the shape of the matter power spectrum from 2DFGRS [11]. The authors attribute the need for the running to the first three CMB multipoles $l = 2; 3; 4$. They introduce power-law spectrum with a cut at large scales and find a non-vanishing cutoff is favored at > 1.5 .

The statistical level of the low CMB multipoles has been discussed widely [15, 16] and many models have been built to achieve the suppressed CMB multipoles [17, 18, 19]. Although the confidence level of spectral index running is not very high, if stands, it would severely constrain inflation model buildings [19, 20, 21] and the single field sneutrino chaotic

inflation model would be in great challenge¹.

Recently we have considered a double inflation model[18, 23]:

$$V(\phi_1, \phi_2) = \frac{1}{2}m_1^2 \phi_1^2 + \frac{1}{2}m_2^2 \phi_2^2; \quad (1)$$

where inflation is driven firstly by the heavier inflaton ϕ_2 , then the lighter field ϕ_1 . But there is no interruption in between. This model solves the problems of flatness etc. and generates a primordial spectrum suppressed at certain small k values. The CMB quadrupole predicted can be much lower than the standard power-law Λ CDM model. Recently, it is shown by Kamionkowski et al.[24] that the cross-correlation between the CMB and an all-sky cosmic-shear map will be enhanced by such a primordial spectrum, and this may be observable at $2 < \ell < 3$ [25]. The suppressed CMB multipoles can also lead to many other observable consequences[26].

In the present work, we consider the case that the two inflaton fields consist of the two lighter sneutrinos, N_1 and N_2 in the minimal supersymmetric seesaw model, while the heaviest one, N_3 , does not contribute to inflation. By fitting the resulted primordial spectrum to the WMAP data in the next section, we get the preferred two sneutrino masses, M_1 and M_2 . We find that the double sneutrino model is more favored than the single sneutrino model at about 1.5 σ level. In section III, we first present our parameterization of the seesaw model and then analyze the implications of this model on the reheating temperature, leptogenesis and lepton flavor violation, etc. We find the reheating temperature, constrained by the gravitino problem [27] to be below $O(10^{10} \text{ GeV})$, gives very strong constraint on the seesaw parameter space and our analysis is greatly simplified then. Different from a random sampling on the 9-dimensional unknown seesaw parameter space in Ref. [3], we can show the seesaw parameter dependence of the predicted lepton flavor violating rate explicitly. Our analysis shows that there is no direct connection between leptogenesis and LFV in this model. Non-thermal leptogenesis is easily to be achieved via the sneutrino inflaton decay. Only hierarchical neutrino mass spectrum at low energy can be produced and the neutrino-less double beta decay [28] can not be explained by the effective Majorana neutrino mass in the model.

¹ Several authors in the literature have fitted WMAP using different codes or adding various CMB and LSS data, they give consistent results[13, 22] but with less hints for running of the spectral index.

II. DOUBLE CHAOTIC SNEUTRINO INFLATION

The evolution of the background fields for double sneutrino inflation is described by the Klein-Gordon equation²:

$$\ddot{\chi}_I + 3H \dot{\chi}_I + V_{,\chi_I} = 0; \quad (2)$$

and the Friedmann equation:

$$H^2 = \left(\frac{\dot{a}}{a}\right)^2 = \frac{8}{3} \frac{G}{2} \dot{\chi}_1^2 + \frac{1}{2} \dot{\chi}_2^2 + V; \quad (3)$$

where $I = 1, 2$, a is the scale factor, the dot stands for time derivative and $V_{,\chi} = \partial V / \partial \chi$. Defining the adiabatic field and its perturbation as [29]:

$$\begin{aligned} \chi &= (\cos \theta) \chi_1 + (\sin \theta) \chi_2; \\ \delta\chi &= (\cos \theta) \delta\chi_1 + (\sin \theta) \delta\chi_2; \end{aligned} \quad (4)$$

with

$$\cos \theta = \frac{\chi_2}{\sqrt{\chi_1^2 + \chi_2^2}}; \quad \sin \theta = \frac{\chi_1}{\sqrt{\chi_1^2 + \chi_2^2}}; \quad (5)$$

The background equations (2) and (3) become

$$\begin{aligned} H^2 &= \frac{8}{3} \frac{G}{2} \left(\frac{1}{2} \dot{\chi}_1^2 + V\right); \\ \ddot{\chi} + 3H \dot{\chi} + V_{,\chi} &= 0; \end{aligned} \quad (6)$$

where $V_{,\chi} = (\cos \theta) V_{,\chi_1} + (\sin \theta) V_{,\chi_2}$. We assume an adiabatic initial condition between the perturbations $\delta\chi_1$ and $\delta\chi_2$:

$$\frac{\delta\chi_1}{\chi_1} = \frac{\delta\chi_2}{\chi_2}; \quad (7)$$

As shown in Ref.[29], if the initial perturbation is adiabatic, it will remain adiabatic on large scales during inflation. In this sense, inflation is equivalently driven by a single inflaton with the effective potential $V(\chi) = V(\chi_1) + V(\chi_2)$. The basic picture of inflation and perturbation in our model is: the heavy inflaton χ_2 rolls slowly down its potential and starts to oscillate when the Hubble expansion rate is around its mass $H \sim M_2$, while χ_1 remains slow rolling and $V(\chi_1)$ comes to dominate the inflation energy density. Hence, inflation is not suspended during the transition.

² To be consistent with the usual convention, in this section, we use χ_I to represent the inflatons, the sneutrinos here, instead of the symbol N_I .

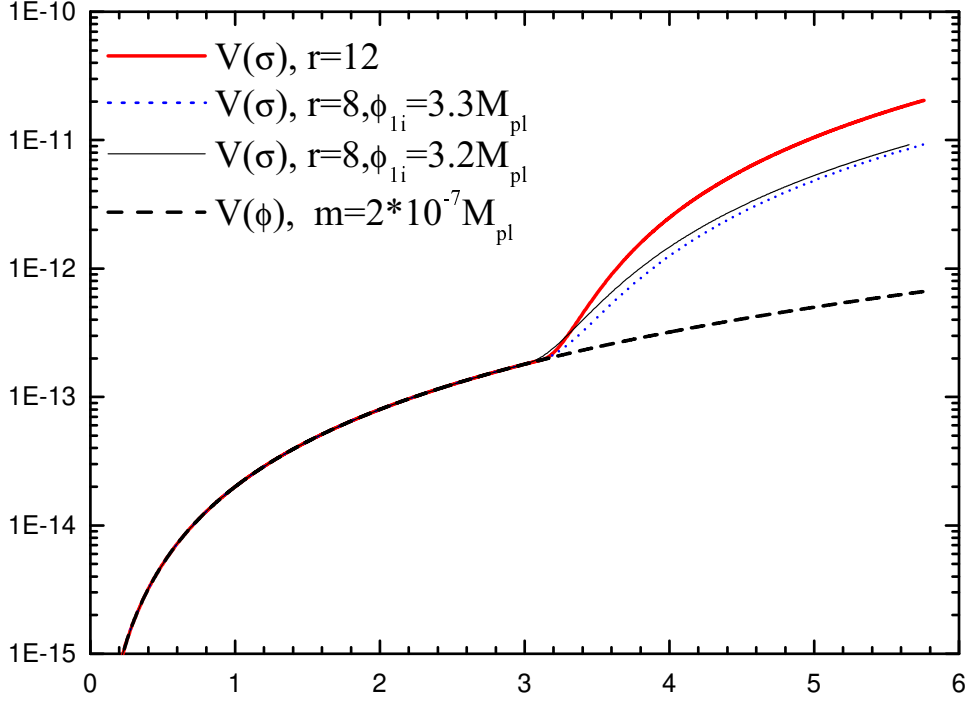


FIG. 1: Effective potentials $V(\sigma)$ together with $V(\phi)$. The horizontal axis is the value of the inflaton ϕ or σ , in unit of M_{pl} . The vertical axis delineates the inflaton potential, in unit of M_{pl}^4 .

The effective potential $V(\sigma)$, as well as the background evolution, is determined by the initial values of ϕ_1, ϕ_2 (i.e. ϕ_{1i} and ϕ_{2i}) and their masses M_1 and M_2 (or equivalently M_1 and $r = M_2/M_1$). As the heavier inflaton oscillates, $j \rightarrow j' a^{\frac{3}{2}}, V(\phi_2) / a^3$, and becomes negligible, one has $\phi_2 = \phi_1$ and $V(\sigma) = V(\phi_1)$. Therefore, the value of ϕ_2 can be set equal to ϕ_1 and they would have the same potentials. In Fig.1 we show the effective potential $V(\sigma)$ as well as $V(\phi)$. $V(\sigma)$ becomes sharper as r increases and the initial value of ϕ_1 would also change the shape of the effective potential.

We notice, from Fig. 1, ϕ_2 achieves a large value during the transition time and the scalar power perturbation is suppressed via the slow-rolling (SR) formula $P_s \propto (\frac{H^2}{2\dot{\phi}})^2$. The SR parameters ϵ and η during the transition are

$$\frac{H}{H^2} = 4 G \left(\frac{\dot{\phi}}{H}\right)^2 \frac{3}{2} \frac{z^2}{z_1 + z_2}; \quad (8)$$

and

$$\frac{H_-}{H_+} = \frac{-\tau_1 + \tau_2}{H(\tau_1 + \tau_2)} \frac{3\tau_2^2}{\tau_1 + \tau_2} : \quad (9)$$

We notice that when τ_2 oscillates, τ_2^2/a^3 , and τ_1 reach their local maximum values. One can also find the maximum value $(\tau_1)_{\max} > (\tau_2)_{\max}$. In the extreme limit when $V(\tau_1)$ is negligible during the transition one has $(\tau_1)_{\max} = 3$ and $(\tau_2)_{\max} = 1.5$. Regarding the fore-mentioned four parameters, the ratio $r = M_2/M_1$ and the initial value of τ_1 , determine the locations and values of $(\tau_1)_{\max}$ and $(\tau_2)_{\max}$. The maximal values are mainly determined by r . If the ratio r is too small (e.g. $1 < r < 3$) the above picture cannot be realized because both fields would take effect during inflation and neither is negligible. While r is too large (e.g. $r > 11$) one gets $1 + \dots < 0$ during the transition and superhorizon effects[30] would take place. The perturbations do get suppressed at some smaller k but enhanced around certain larger k values. Under such circumstances the whole effect might be negative to achieve small CMB TT quadrupole. The need that $P_S(k)$ be suppressed at small k requires some tuning of the initial value of τ_1 . M_1 determines the amplitude of the perturbation and is normalized by the current observations. The initial value of τ_2 is arbitrary with a weak prior to provide enough number of e-folding to solve the flatness problem.

As our model parameters lie in the region where SR approximation does not work well, we calculate the primordial scalar and tensor spectra using mode by mode integrations[18, 20, 31]. We denote the scale where P_S arrives around its local maximum as k_f and tune the initial τ_1 to get $N(k_f) = 55$. In Fig. 2 we show the numerical results of the scalar and tensor spectra for $r = 3.5, 9$ and 11.5 . One can see that, for $r = 3.5$, the spectra is almost featureless while well suppressed scalar spectra have been generated for $r = 9$ and 11.5 . For the example of $r = 11.5$ P_S is enhanced around k_f due to the superhorizon contributions[30].

We then fit the resulting primordial spectra to the current WMAP TT and TE data. As shown in Refs.[32, 33], in such inflation models one cannot know the exact values of k_f due to the uncertainty in the details of reheating. So $\ln k_f$ is another parameter in our model. Our fitting is similar to Ref.[18]: We fix $\Omega_b h^2 = 0.022$, $\Omega_m h^2 = 0.135$, $\Omega_c = 0.17$, $\Omega_{tot} = 1$ [15] and set Ω_{tot} and $\ln k_f$ as free parameters in our fit. Denoting $k_c = 7:0 \quad 70:=3=10^5$ $1:6 \quad 10^3 \text{ Mpc}^{-1}$, we vary grid points with ranges $[0.68;0.77]$, and $[3;5]$ for $\ln k_f$ and $\ln(k_f/k_c)$, respectively. M_2/M_1 varies from 3.5 to 12 in step of 0.5. At each point in the grid we use subroutines derived from those made available by the WMAP team to evaluate

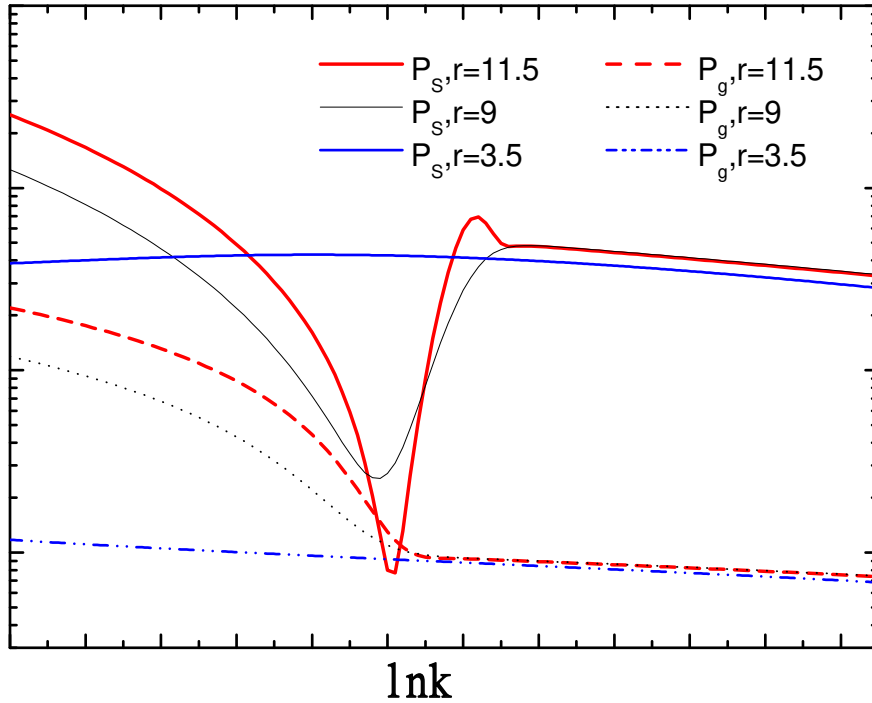


FIG. 2: Primordial scalar P_s and tensor spectra P_g for $r = 3.5, 9$ and 11.5 . The overall amplitude can be normalized by WMAP.

the likelihood with respect to the WMAP TT and TE data [34]. The overall amplitude of the primordial perturbations has been used as a continuous parameter.

In Fig. 3 we plot the resulting χ^2 values as functions of r and $\ln(k_f=k_c)$. The contours shown are for χ^2 values giving 1, 2, and 3 contours for two parameter Gaussian distributions. As the location is rather hard to be fixed at exactly $N(k_f) = 55$, the figure is not very smooth as expected. Our main intention is to see how the primordial spectrum with a feature is favored by WMAP. This can be also seen in the one-dimensional marginalized distribution of $\ln(k_f=k_c)$ for each r . To see clearly how the feature is favored, we do not marginalize over r and show some of them in Fig. 4. For $r = 3.5$, $k_f = 0$ is favored and when $r = 7$, $\ln(k_f=k_c) = 3$ is favored at around 2×10^4 . $k_f = 0$ is excluded at less than 1% for $r = 4.5$ where P_s is not suppressed enough around k_f . While for $r > 11$, P_s is enhanced around k_f and although nonzero k_f is favored for shown examples, $k_f = 0$ is excluded at less

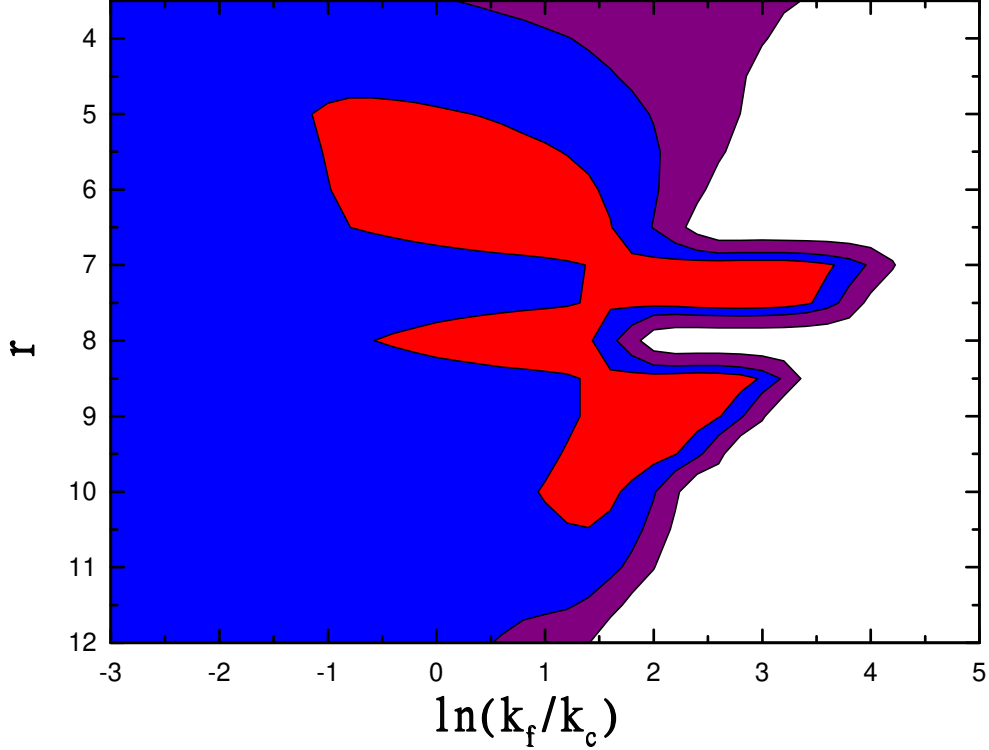


FIG. 3: Two-dimensional contours in the r vs $\ln(k_f/k_c)$ plane for our grids of model $k_c = 1.6 \times 10^3 \text{ Mpc}^{-1}$. The regions of different color show 1 σ , 2 σ and 3 σ confidence respectively.

than 1. We find that, for $6 < r < 10$, nonzero k_f is favored at > 1.5 . For the investigated parameter space with $3.5 < r < 12$ we have $P_S(0.05 \text{ Mpc}) = 2.46 - 2.59 \times 10^9$ at 2 σ level. This gives $M_1 = 1.7 - 10^3 \text{ GeV}$.

A detailed analysis gives the e-folds number $N(k)$ before the end of inflation [32, 33]:

$$N(k) = 60.56 - \ln h - \ln \frac{k}{a_0 H_0} - \ln \frac{10^{16} \text{ GeV}}{(k)^{1=4}} + \ln \frac{(k)^{1=4}}{1=4} - \frac{1}{3} \ln \frac{1=4_{\text{end}}}{1=4_{\text{RH}}}; \quad (10)$$

where (k) , $_{\text{end}}$ denote the inflation potential at $k = aH$ and at the end of inflation respectively, $_{\text{RH}}$ is the energy density when reheating ends, resumming a standard big bang evolution. Since in our case there is a preferred scale $\ln(k_f=k_c)$ while $N(k_f)$ is fixed around 55, the reheating energy may be determined by the current observations. However, one can see that the location of k_f is mainly determined by the initial value of $_{1}$. Once the initial $_{1}$ changes, $N(k_f)$ will change and the resulting $_{\text{RH}}$ would be different. We show the case

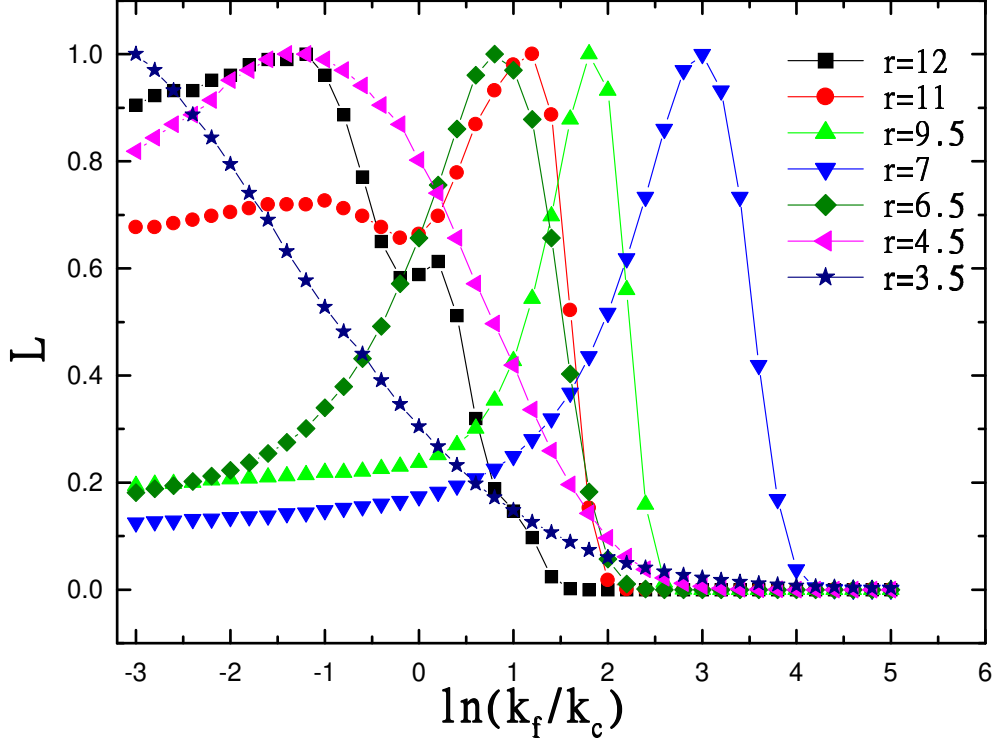


FIG. 4: One-dimensional marginalized distributions of $\ln(k_f/k_c)$ for $r = 3.5, 4.5, 6.5, 7, 9.5, 11$ and 12 .

in Fig. 5 as an example. For $r = 8$, $\beta_i = 3.2$ and $3.3M_{pl}$ lead to $N(k_f) = 54.34$ and 59.06 respectively. We get $P_S = 2.5 \times 10^9$ at $0.05 M_{pc}^{-1}$, the resulting $\ln(k_f/k_c) = (1.7; 1.3)$ and $(0.1; 1.9)$ at 2 respectively. We also have $h = 0.73$, $\frac{1}{4}(0.05 M_{pc}) = 1.8 \times 10^3 M_{pl}$ and $\frac{1}{4}_{end} = 5.1 \times 10^4 M_{pl}$. Taking these to the models we get $\frac{1}{4}_{RH} = (8.5 \times 10^4 \text{ GeV}; 6.9 \times 10^6 \text{ GeV})$ and $(2.6 \times 10^3 \text{ GeV}; 5.8 \times 10^5 \text{ GeV})$ at 2 for the two different β_i . Therefore, the reheating temperature is fully correlated with initial β_i in this model.

We get our minimum $\chi^2 = 1429.1$ when $r = 8.5$ and $\ln(k_f/k_c) = 2.4$. When compared with the standard power-law CDM model, we have minimum $\chi^2 = 1432.7$ and $\chi^2 = 3.6$. For the single field chaotic inflation we get minimum $\chi^2 = 1432.9$, with $\chi^2 = 3.8$. However, in the sneutrino inflation, we have to set $\frac{1}{4}_{RH} < 10^{10} \text{ GeV}$ due to the gravitino problem [27]. In this case, we get $N(k_c) < 55.5$ and minimum $\chi^2 = 1433.2$, which gives $\chi^2 = 4.1$. In addition, there are only two parameters, the mass and $\ln(k_f/k_c)$, in the

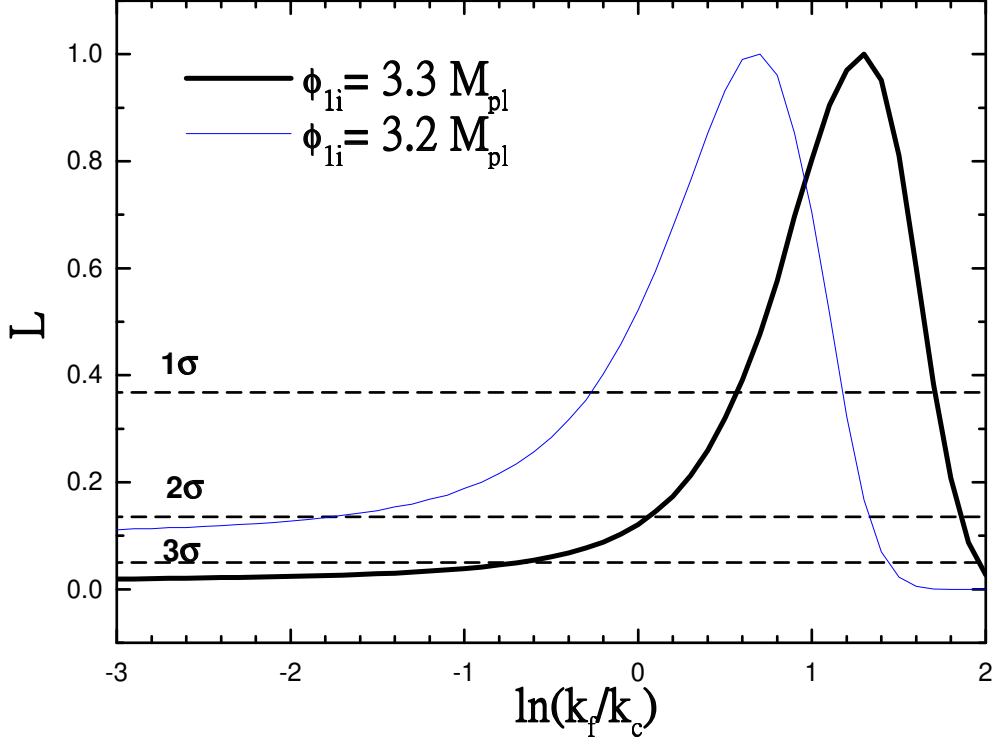


FIG. 5: One dimensional likelihoods of $r=8$, $\phi_{li} = 3.2$ and $3.3 M_{pl}$.

single field sneutrino inflation model. This indicates our double sneutrino inflation is favored at 1.5 by WMAP than the single field sneutrino inflation. In Fig. 6 we show the resulting CMB TT multipoles and two-point temperature correlation function for single and double field sneutrino inflation in our parameter space. One can see that the resulting CMB TT quadrupole and the correlation function at $l > 60$ are much better suppressed in the double sneutrino inflation than in the single sneutrino model. In fact, the spectrum of the single field sneutrino inflation is equivalent to that in our double case with $r = 1$ and $\phi_{li} = \phi_{2i}$. In this sense we get $6 < r < 10$ is favored at > 1.5 ($2 < \chi^2 < 2.3$) than $r = 1$ in double sneutrino inflation.

Finally, it is worth mentioning that we have also considered a double inflation model with

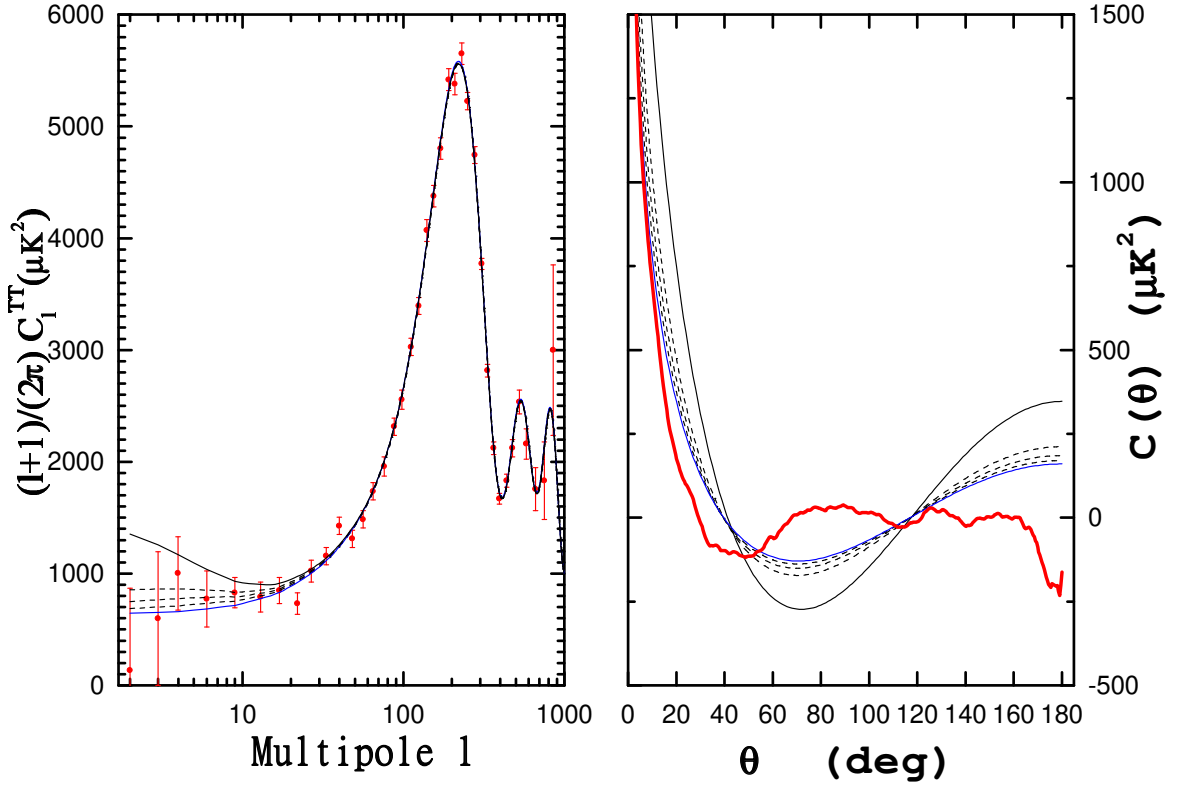


FIG . 6: C M B anisotropy and two-point temperature correlation function for single and double e ld sneutrino in ation . Left: From left top to bottom , the lines stand for single sneutrino in ation, double sneutrino in ation with $\ln(k_f=k_c) = 3.0, 3.2, 3.4$ and 3.6 . r is fixed at 8.5 . Right: From right top to bottom , the lines stand for single sneutrino in ation, double sneutrino in ation with $\ln(k_f=k_c) = 3.0, 3.2, 3.4$ and 3.6 and the W M A P released data.

quartic potential³

$$V(\phi_1; \phi_2) = \frac{1}{2} \phi_1^2 + \frac{1}{2} \phi_2^2 + \dots \quad (11)$$

As we know n, the quartic potential ⁴ is disfavored by the current W M A P and LSS observations, because it has a larger tensor perturbation. Peiris et al. [10] x the number of e-folding at 50 and nd ⁴ in ation model is excluded at more than 3 by W M A P and 2DFGRS data. W M A P alone excludes ⁴ in ation at more than 99% con dence level

³ The quartic term of sneutrino is absent in the minimal supersymmetric seesaw mechanism . These terms can arise if the RH neutrino Majorana mass is produced in the superpotential $N N$, with another super e ld whose vacuum expectation value generates the Majorana mass.

when $N = 50$. The discrepancy between the theoretical predictions and observations comes mainly from the contributions of small CMB multipoles. In the double inflation quartic model, the CMB quadrupoles can also be well suppressed and the model is also favored by WMAP. We fix $N(k_f) = 50$ and run two codes, one with $n_{\text{run}} = 6400$ and the other with $n_{\text{run}} = 3600$ and fit the primordial scalar and tensor spectra to WMAP TT and TE data. We get minimum $\chi^2 = 1427.9$ and 1428 respectively. They work better than the double quadratic sneutrino inflation. Reheating temperature in this case cannot be restricted from WMAP, as shown in Ref.[35].

III. PHENOMENOLOGY

In the minimal seesaw mechanism, the right-handed sector is least known. However, in the double sneutrino inflation model, two neutrino masses M_1 and M_2 are constrained by the WMAP as shown in the previous section. In the following, we will study the phenomenological implications of this model, including the reheating temperature, leptogenesis, lepton flavor violation and neutrinoless double beta decay.

A. Parameterization of the minimal seesaw model

In this subsection we present our convention and parameterization of the minimal supersymmetric seesaw model. At the energy scales above the RH neutrino masses, the superpotential of the lepton sector is given by

$$W = Y_L^{ij} \hat{H}_1 \hat{L}_i \hat{E}_j + Y_N^{ij} \hat{H}_2 \hat{L}_i \hat{N}_j + \frac{1}{2} M_R^{ij} \hat{N}_i \hat{N}_j + \hat{H}_1 \hat{H}_2 ; \quad (12)$$

where Y_L and Y_N are the charged lepton and neutrino Yukawa coupling matrices, respectively, M_R is the Majorana mass matrix for the right-handed neutrinos, with i and j being the generation indices.

Generally, Y_L and Y_N can not be diagonalized simultaneously. This mismatch leads to the lepton flavor violating (LFV) interactions. The three matrices Y_L , Y_N and M_R can be diagonalized by

$$Y_L = U_L^Y Y_L U_R ; \quad (13)$$

$$Y_N = V_L^Y Y_N V_R ; \quad (14)$$

$$M_R = X V_R^T M_R V_R X^T ; \quad (15)$$

respectively, where $U_{L,R}$, $V_{L,R}$ and X are all unitary matrices.

We can define the lepton flavor mixing matrix V , the analog to the Kobayashi-Maskawa matrix V_{KM} in the quark sector, as

$$V = U_L^Y V_L ; \quad (16)$$

V is determined by the left-handed mixing of the Yukawa coupling matrices Y_L and Y_N , and only exists above the energy scales M_R . We will see below that this matrix determines the LFV effects in the supersymmetric seesaw model at low energies.

We then rotate the bases of \hat{L} , \hat{E} and \hat{N} to make both Y_L and M_R diagonal. On this basis, Y_N can be written in a general form as

$$Y_N = V Y X^T ; \quad (17)$$

By adjusting the phases of the superfields, V is a CKM-like mixing matrix with one physical CP phase, and X has the form

$$X = \begin{pmatrix} e^{i\alpha} & & & \\ & e^{i\beta} & & \\ & & e^{i\gamma} & \\ & & & e^{i\delta} \end{pmatrix} X' \begin{pmatrix} e^{i\theta} & & & \\ & e^{i\phi} & & \\ & & e^{i\psi} & \\ & & & e^{i\omega} \end{pmatrix} ; \quad (18)$$

where $\alpha, \beta, \gamma, \delta, \theta, \phi, \psi, \omega$ are Majorana phases and X' is a CKM-like mixing matrix with another Dirac CP phase. It is then easy to count that there are 18 parameters to parameterize the minimal seesaw mechanism, which include 6 Yukawa coupling constants (or mass) eigenvalues in Y_N and M_R , 6 mixing angles and 6 CP phases in V and X .

At low energies, the heavy RH neutrinos are integrated out and the Majorana mass matrix for the left-handed neutrinos is given by

$$m = m_N \frac{1}{M_R} m_N^T ; \quad (19)$$

where $m_N = Y_N v \sin \theta$ is the neutrino Dirac mass matrix, with v being the vacuum expectation value (VEV) of the Higgs boson. m can be diagonalized by

$$U^Y m U = m ; \quad (20)$$

where $U = U \text{diag}(1; e^{i\alpha}; e^{i\beta})$ is the MNS mixing matrix [36], with α, β being low energy Majorana CP phases. U describes the neutrino mixing at low energies, which is different from the high energy mixing matrix V defined in Eq. (16). From Eq. (19) we can see that m is related to all the 18 seesaw parameters. However, measuring m at low energy only determines 9 of the 18 seesaw parameters. We will see below that leptogenesis and lepton flavor violation are related to different combinations of the 18 seesaw parameters and can provide different information to determine the seesaw parameters from the θ -oscillation and LFV observations.

We can rewrite the seesaw formula Eq. (19) in another form

$$U \frac{m}{m} U \frac{m}{m}^T = V m_N X^T \frac{1}{M_R} \oplus V m_N X^T \frac{1}{M_R} A^T ; \quad (21)$$

from which m_N can be solved in terms of the left- and right-handed neutrino masses,

$$m_N = V \frac{m}{m} \hat{O}^T \frac{m}{m} M_R X ; \quad (22)$$

where \hat{O} is an arbitrary orthogonal 3×3 matrix [37] and $V^0 = U^Y V$. In the above equation we have absorbed all the 6 Majorana CP phases in the diagonal eigenvalue matrices: two low energy Majorana phases, α, β , are absorbed by $\frac{m}{m}$ and the four high energy Majorana phases, $\theta_1, \theta_2, \theta_3, \theta_4$, are absorbed by m_N and M_R . We will use this equation repeatedly in the following discussions.

B. The reheating temperature

The lightest sneutrino N_1 begins to oscillate when the Hubble expansion rate $H = M_1$ and decays at $H = \Gamma_{N_1}$. The Universe is then reheated by the relativistic decay products. The reheating temperature is approximately determined by

$$T_{RH} = \frac{90}{2g} \left(\frac{1}{4} \right)^{\frac{1}{4}} \frac{m}{m} M_P ; \quad (23)$$

where g is the number of the effective relativistic degrees of freedom in the reheated Universe, $M_P = \sqrt{\frac{3}{8\pi G_N}}$, 2.4×10^{18} GeV is the Planck scale, and

$$\Gamma_{N_1} = \frac{1}{4} (Y_N^Y Y_N)_{11} M_1 ; \quad (24)$$

right-handed (s)neutrino decouples from the other two generations and no lepton number asymmetry can be induced when it decays. However, the tiny mixing has no effect on lepton flavor violation and we can ignore them safely when discussing LFV.)

From Eq. (29) we can estimate that

$$m_1 \begin{cases} \lesssim 2: & 10^{10} \text{ eV}; \text{ for } T_{RH} = 10^{10} \text{ GeV}; \\ \gtrsim 2: & 10^{12} \text{ eV}; \text{ for } T_{RH} = 10^9 \text{ GeV}; \end{cases} \quad (31)$$

This estimation is correct when the last two terms are much smaller than the first one in the second line of Eq. (29), or, equivalently, the Y_1 term dominates the others in Eq. (26). In the following discussion for leptogenesis we will see that this is a quite natural situation.

C. Leptogenesis

Since the reheating temperature, T_{RH} , is far below the lightest RH (s)neutrino mass, M_1 , leptogenesis arises dominantly from direct cold sneutrino decays, with negligible thermal wash-out effects. In this case, the baryon asymmetry is given by [38]

$$Y_B = \frac{n_B}{s} = a \frac{3}{4} \frac{T_{RH}}{M_1}; \quad (32)$$

where $a = 8/23$ is the ratio of baryon to lepton asymmetry balanced by the "sphaleron" process. In order to produce the observed baryon asymmetry in the Universe, $Y_B \approx 10^{10}$, we require the sneutrino decay asymmetry $\epsilon_1 \approx 10^6$. The asymmetry ϵ_1 is given by

$$\epsilon_1 = \frac{3}{16} \frac{1}{(Y_N^y Y_N)_{11}} \sum_{i=2,3} X_i \text{Im} \left((Y_N^y Y_N)_{1i} \right) \frac{M_1}{M_i}; \quad (33)$$

Using the expression for X in Eq. (28) and the large hierarchy between Y_1 and Y_2, Y_3 we get

$$\begin{aligned} (Y_N^y Y_N)_{12} &= (g_2 Y_2^2 + g_1 s_3 Y_3^2) e^i; \\ (Y_N^y Y_N)_{13} &= (g_3 Y_2^2 + g_1 Y_3^2) e^i; \end{aligned} \quad (34)$$

We will discuss two simple cases to illustrate some quantitative features of the seesaw parameters required by leptogenesis. We will see that, in Eq. (26), the Y_2 and Y_3 terms should be smaller than the Y_1 term in order to produce the lepton number asymmetry at the correct order.

Case I, $s_3^2 Y_3^2 \ll s_2^2 Y_2^2$

In this case the expression for j_1 is simplified as

$$j_1 = \frac{3}{16} \frac{1}{(Y_N^Y Y_N)_{11}} (s_2 Y_2^2)^2 \sin 2 \frac{M_1}{M_2} + (s_2 s_3 Y_2^2)^2 \sin 2 \frac{M_1}{M_3} - 10^4 \frac{s_2^2 Y_2^2}{Y_1^2 + s_2^2 Y_2^2} \sin 2 \quad ; \quad (35)$$

When deriving the second line we have assumed that $s_3^2 Y_3^2$ and $s_2^2 Y_2^2$ are of the same order and $\frac{M_1}{M_3} \ll \frac{M_1}{M_2} \ll Y_2 \ll 0.1$ and $s_1^2 Y_3^2 \ll s_2^2 Y_2^2$. If the CP phases are of order 1, $s_2^2 Y_2^2 = Y_1^2$ should be at the order of about 10^2 . Actually, this case corresponds to the maximal asymmetry given by $j_1^{\text{max}} \approx \frac{3}{16} \frac{M_1}{v^2} \frac{m_{\text{sol}}^2}{v^2} \approx 10^4$ [39]. In this case, the CP phase $\phi_2 = (Y_N^Y Y_N)_{11}$, has to be at the order of $O(10^2)$.

Case II, $s_3^2 Y_3^2 \gg s_2^2 Y_2^2$

In this case we can simplify the expression for j_1 as

$$j_1 = \frac{3}{16} \frac{1}{(Y_N^Y Y_N)_{11}} (s_1 s_3 Y_3^2)^2 \sin 2 \frac{M_1}{M_2} + (s_1 Y_3^2)^2 \sin 2 \frac{M_1}{M_3} - 10^3 \frac{s_1^2 Y_3^2}{Y_1^2 + s_1^2 Y_3^2} (\sin 2^0 + \sin 2^{-0}) ; \quad (36)$$

where we have used the fact that $s_3^2 Y_3^2 \gg s_2^2 Y_2^2$ if τ is of order 1, $s_1^2 Y_3^2 \gg s_2^2 Y_2^2$ and $\theta = 0$, $\phi = 0$. Similar to Case I, we get that $s_1^2 Y_3^2 = Y_1^2$ should be at the order of 10^3 if the CP phases are of order 1. In this case, the maximal asymmetry is $j_1^{\text{max}} \approx \frac{3}{16} \frac{M_1}{v^2} \frac{m_{\text{atm}}^2}{v^2} \approx 10^3$.

Certainly, it is possible that the contributions to $(Y_N^Y Y_N)_{11}$ from Y_2 and Y_3 in Eq. (26) are of the same order. In this case we also expect that these values be correct as an estimate of the order of magnitude, i.e., $s_1^2 Y_3^2 \ll s_2^2 Y_2^2 \ll Y_1^2$. This analysis justifies our guess in the last subsection that the Y_1 term gives the dominant contribution in the process of reheating the Universe. Conversely, if the Y_2 or Y_3 term gives dominant contribution, the CP phases have to be fine-tuned to the order of 10^{-2} and 10^{-3} respectively, in order not to create too much lepton number asymmetry and m_{ν} in Eq. (31) will be even smaller.

D. Lepton flavor violation and muon anomalous magnetic moment

We have shown that leptogenesis is associated with the high energy mixing angles and CP phases in the unitary matrix X . Generally, leptogenesis has no direct relation with the

low energy neutrino phenomena. However, another interesting phenomena | the charged lepton flavor violating decays | predicted by this sneutrino in aton model, can provide constraints on the seesaw model's parameter space. The muon anomalous magnetic moment is also considered to constrain the SUSY parameters.

In a supersymmetric model, the present experimental limits on the LFV processes has put very strong constraints on the soft supersymmetry breaking parameters, with the strongest constraints coming from the process $\mu \rightarrow e \gamma$ ($BR(\mu \rightarrow e \gamma) < 1.2 \times 10^{-11}$ [40]). It is a usual practice to assume universal soft SUSY breaking parameters m_0 , $m_{1=2}$ and A_0 at the SUSY breaking scale (We take it the GUT scale here) to suppress the LFV effects. However, since there are LFV interactions in the seesaw models, the lepton flavor violating off-diagonal elements of $(m_{\tilde{L}}^2)_{ij}$, the slepton doublet soft mass matrix, and $(A_e)_{ij}$, the lepton soft trilinear couplings, can be induced when running the renormalization group equations (RGEs) for $m_{\tilde{L}}^2$ and A_e between M_{GUT} and M_R .

The off-diagonal elements of $(m_{\tilde{L}}^2)_{ij}$ and $(A_e)_{ij}$ can be approximately given by

$$m_{\tilde{L}}^2{}_{ij} = \frac{1}{8} \frac{1}{2} (Y_N Y_N^Y)_{ij} (3 + a^2) m_0^2 \log \frac{M_{GUT}}{M_R}; \quad (37)$$

$$(A_e)_{ij} = \frac{1}{8} \frac{1}{2} (Y_N Y_N^Y)_{ij} a m_0 \log \frac{M_{GUT}}{M_R}; \quad (38)$$

where $A_0 = a m_0$ is the universal trilinear coupling at M_{GUT} . Using Eq. (17) we have

$$(Y_N Y_N^Y)_{ij} = (V (Y_N)^2 V^Y)_{ij} = V_{i2} V_{j2} Y_2^2 + V_{i3} V_{j3} Y_3^2; \quad \text{for } M_{GUT} > Q > M_3 \quad (39)$$

$$= \sum_{k=1,2}^X (V Y_N X^T)_{ik} (X Y_N V^Y)_{kj} \\ = \sum_{l,m=2,3} V_{il} V_{jm} Y_l Y_m (X_{lm} - X_{3l} X_{3m}); \quad \text{for } M_3 > Q > M_2; \quad (40)$$

The numerical result shows that, since the mixing angles in X are all small, the LFV effects are only sensitive to the left-handed mixing matrix V , while leptogenesis only relies on the right-handed mixing matrix X . Thus, there are no direct relation between the two phenomena in principle.

We have solved the full coupled RGEs numerically from the GUT scale to M_Z scale. At the energy scales below M_2 we solve the RGEs for MSSM and below M_{SUSY} the RGEs return to those of the SM.

In principle, only 9 of the 18 seesaw parameters are determined in our model, i.e., $m_{\tilde{\nu}_i}$, M_i and 3 low energy neutrino mixing angles. In order to predict the branching ratio of the

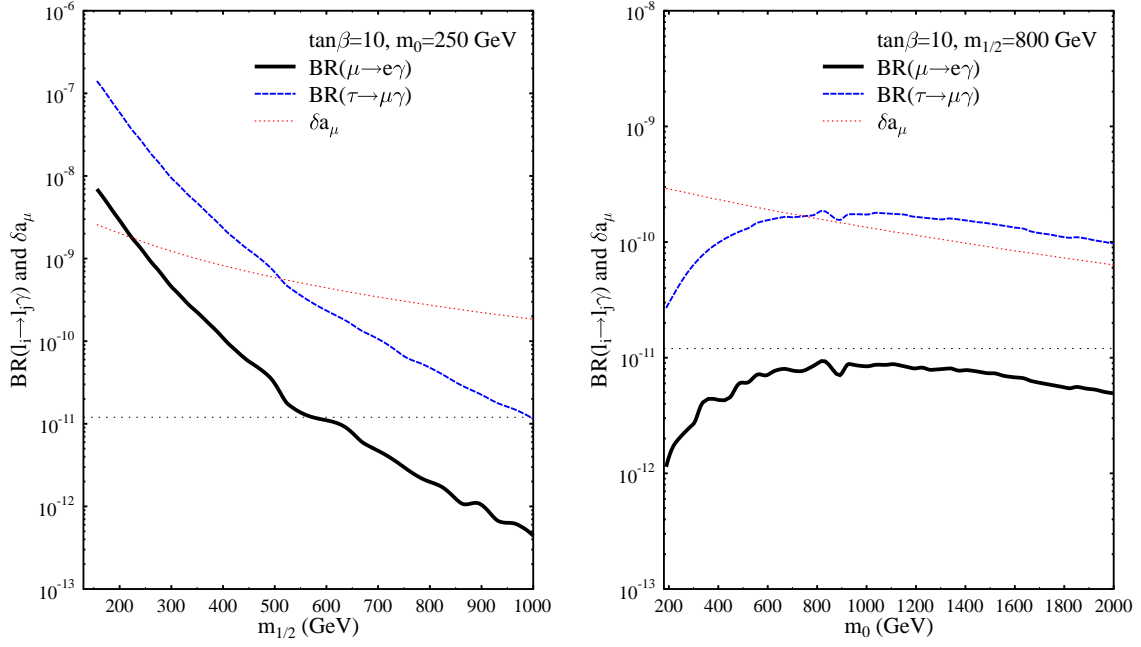


FIG .7: $BR(l_i \rightarrow l_j \gamma)$ and δa_μ as a function of $m_{1/2}$ and m_0 in the left and right panels respectively. $\tan \beta = 10$, $A_0 = 0$ and $\mu > 0$ are fixed. We take $m_0 = 250 \text{ GeV}$ for the left panel and $m_{1/2} = 800 \text{ GeV}$ for the right panel. The seesaw parameters are taken as $M_T = -4$, $\theta_i = 0$, $\theta_{13} = 0.05$ and $M_3 = 1 \cdot 10^{15} \text{ GeV}$.

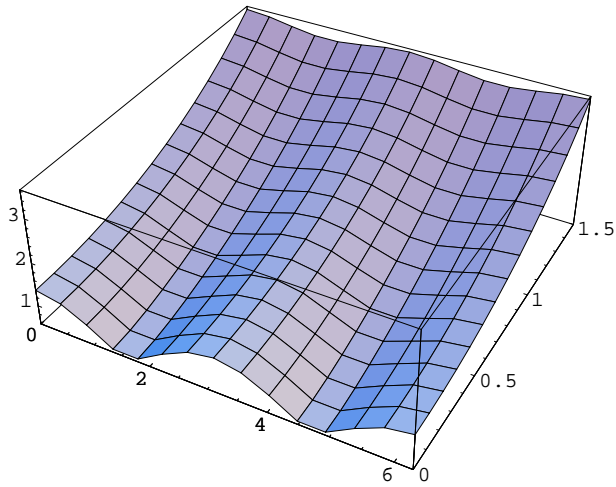


FIG .8: Y_3 as function of θ_T for $\text{Re } \theta_T = 0 \dots 2$ and $\text{Im } \theta_T = 0 \dots 1.5$.

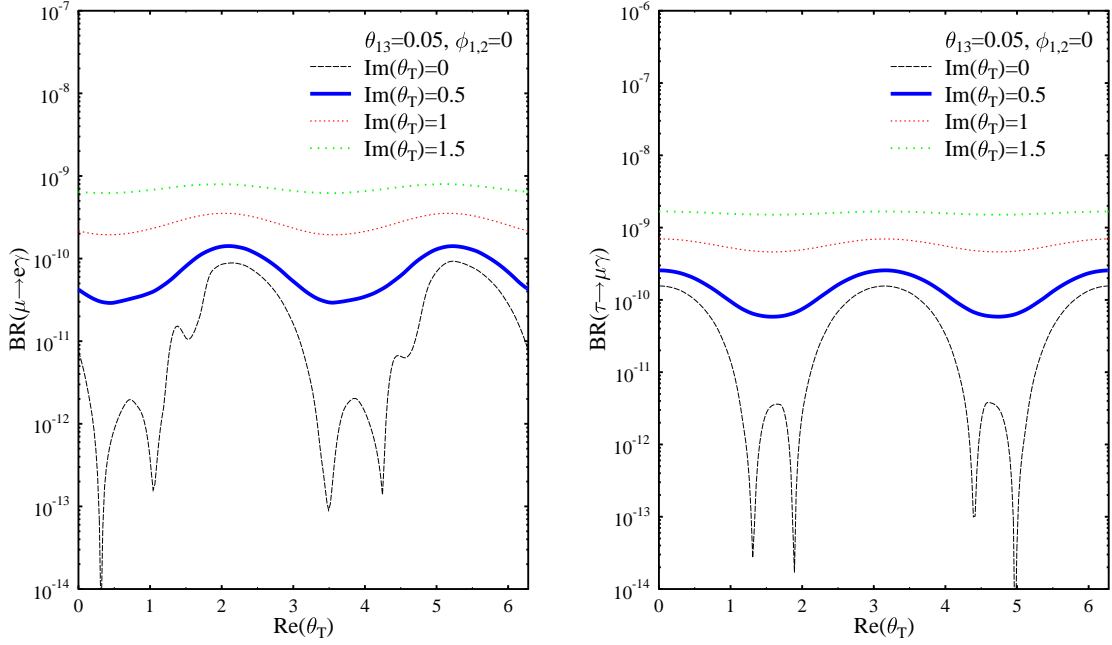


FIG. 9: $BR(\mu \rightarrow e\gamma)$ (Left) and $BR(\tau \rightarrow \mu\gamma)$ (Right) as function of $\text{Re}(\theta_T)$ for $\text{Im}(\theta_T) = 0; 0.5; 1; 1.5$. We set $\theta_{13} = 0.05$, $\phi_{1,2} = 0$ and $M_3 = 1 \cdot 10^{15} \text{ GeV}$.

determined by θ_T . In Fig. 8 we show Y_3 as function of $\text{Re}(\theta_T)$ and $\text{Im}(\theta_T)$. Both the real and imaginary part influence the ratio between Y_2 and Y_3 . Since Y_3 increases almost linearly with $\text{Im}(\theta_T)$, we expect $BR(l_i \rightarrow l_j \gamma)$ also increase with $\text{Im}(\theta_T)$.

In Fig. 9, we plot $BR(\mu \rightarrow e\gamma)$ and $BR(\tau \rightarrow \mu\gamma)$ as function of $\text{Re}(\theta_T)$ on the left and right panels respectively. For $\text{Im}(\theta_T) = 0.5$, $BR(\mu \rightarrow e\gamma)$ has been greater than the experimental limit.

In Fig. 10, $BR(l_i \rightarrow l_j \gamma)$ is drawn as function of θ_{13} . We can see $BR(\mu \rightarrow e\gamma)$ is very sensitive to θ_{13} , while $BR(\tau \rightarrow \mu\gamma)$ is insensitive to θ_{13} . The behavior in this figure is understood if we notice that the flavor mixing between the first and the second generations is nearly proportional to $V_{13}V_{23}Y_3^2$, where $V_{13} = (U)_{12}V_{23}^0 + (U)_{13}V_{33}^0$. The two terms are added constructively or destructively, depending on the sign of θ_T . When we set $\theta_{12} = 0$, the branching ratio of $\mu \rightarrow e\gamma$ increases rapidly with θ_{13} , independent of the value of θ_T .

In Fig. 11, we plot $BR(l_i \rightarrow l_j \gamma)$ as function of θ_1 , which determines the relative phase between U and V^0 . The behavior in the figure is easy to understand. We also examined that $BR(l_i \rightarrow l_j \gamma)$ is indeed independent of θ_2 , as we expected.

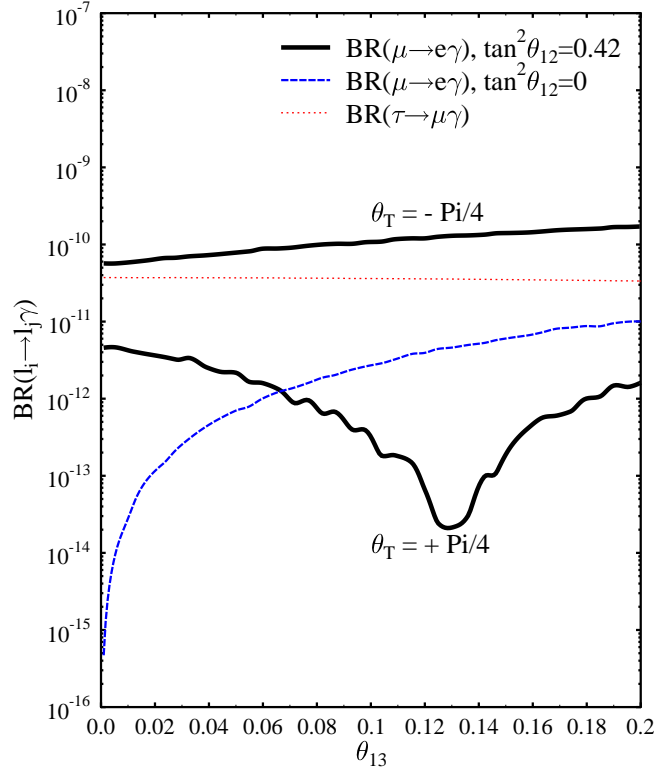


FIG. 10: $BR(l_i \rightarrow l_j \gamma)$ as function of θ_{13} . We $x_i = 0$ and $M_3 = 1 \cdot 10^{15} \text{G eV}$.

Finally, we plot $BR(l_i \rightarrow l_j \gamma)$ as function of M_3 . $BR(l_i \rightarrow l_j \gamma)$ increases with M_3 at first, because it makes $Y_{2,3}$ larger. However, when M_3 is as large as 10^{16}G eV , which is too close to M_{GUT} , the integration distance $\log \frac{M_{\text{GUT}}}{M_3}$ becomes too small and the branching ratio decreases. Although below M_3 LFV is still produced, see Eq. (40), the effects are small, since the contribution from Y_2^2 is small, due to $Y_2^2 \ll Y_3^2$. The Y_3 coupling contributes to the LFV below M_3 through the mixing, $Y_3^2 \tilde{X}_{23}^2$, which is also small due to the small mixing element.

We have omitted $BR(\mu \rightarrow e \gamma)$ in all the figures because the predicted branching ratio is much smaller than the present experimental limit.

E. Neutrinoless double beta decay

From the above discussion we know that it is impossible to produce degenerate solution for the left-handed neutrino masses in this model. It is easy to estimate that $\langle m \rangle_{ee} =$

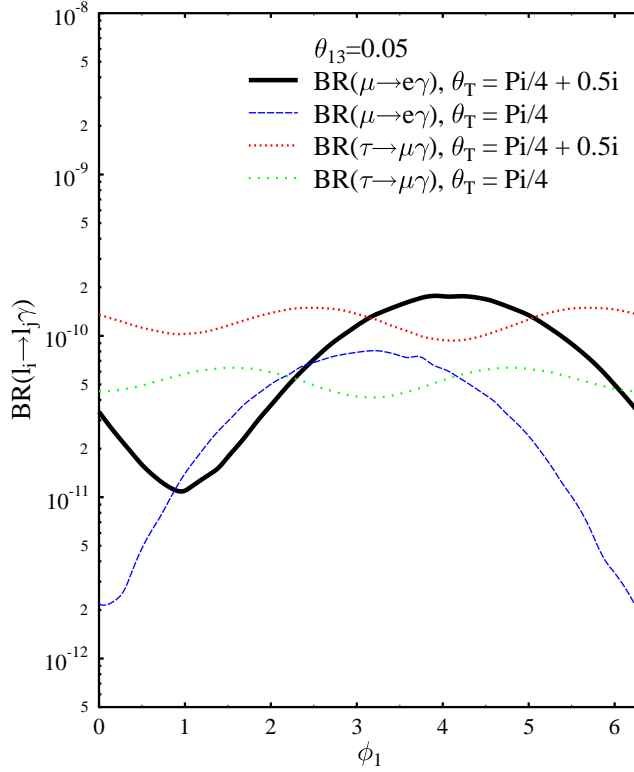


FIG. 11: $BR(l_i \rightarrow l_j \gamma)$ as function of ϕ_1 . We $\theta_{13} = 0.05$, $\theta_{21} = 0$ and $M_3 = 1 \cdot 10^{15} \text{ GeV}$.

(2–4) 10^3 eV , depending on the value of U_{e3} . So, in this sneutrino-inflaton model, it is hard to account for the neutrinoless double beta decay experimental signal [28].

IV. SUMMARY AND DISCUSSIONS

We have considered a double-sneutrino inflation model within the minimal supersymmetric seesaw model. With the mass ratio $6 < r < 10$ and the lighter sneutrino $M_1 = 1.7 \cdot 10^3 \text{ GeV}$, the model predicts a suppressed primordial scalar spectrum around the largest scales which is favored at > 1.5 . The predicted CMB TT quadrupole is much better suppressed than the single sneutrino model and the preference level by the WMAP first year data is about 1.5. Double quartic inflation can also work very well in light of WMAP observations.

We then have studied the phenomenological implications of this model. The seesaw parameters are constrained by both particle physics and cosmological observations. The strongest constraint comes from the required reheating temperature by the gravitino prob-

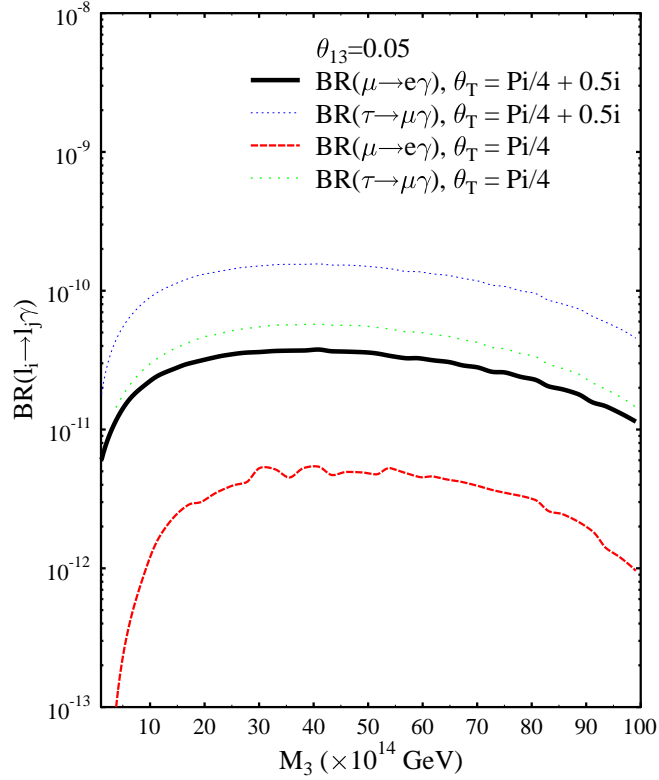


FIG. 12: $BR(l_i \rightarrow l_j \gamma)$ as function of M_3 for $\theta_T = \pi/4 + 0.5i$ and $\theta_T = \pi/4$. We $\theta_{13} = 0.05$ and $\theta_{12} = 0$.

lem. To some extent, no tuning is needed to satisfy this constraint, which means that the right-handed mixing angles θ_{12} and θ_{13} are much smaller than the mass hierarchy of the right-handed neutrinos. Further, the mass of the lightest left-handed neutrino should be at the order of 10^{10} eV, much smaller than the other two light neutrinos.

Leptogenesis arises from the decays of the cold inflaton into the lightest sneutrino. It is easy to account for the observed quantity of the baryon number asymmetry in the Universe by adjusting the seesaw parameters.

This model gives definite predictions on the lepton flavor violating decay rates. In most parameter space, the branching ratio of $\tau \rightarrow \mu e \gamma$ is near or exceeds the present experimental limit. However, the branching ratio of $\tau \rightarrow \mu \gamma$ is at the order of about $10^{10} - 10^9$, which is far below the current experimental limit. Furthermore, in the appropriate range of SUSY parameter space where LFV constraints are satisfied, the SUSY can only enhance the muon anomalous magnetic moment at the amount of $(2 - 3) \times 10^{10}$.

This model can not predict a degenerate light neutrino spectrum. The observed signal of neutrinoless double beta decay, if finally verified, can not be explained by the effective Majorana neutrino mass in this model.

Acknowledgments

We thank Z. Z. Xing for helpful discussions. We acknowledge the using of CMBFAST program [43, 44]. This work is supported by the National Natural Science Foundation of China under the grant No. 10105004, 19925523, 10047004 and also by the Ministry of Science and Technology of China under grant No. NKBRSG 19990754.

-
- [1] A. Guth, *Phys. Rev. D* 23, 347 (1981); A. Linde, *Phys. Lett. B* 108, 389 (1982). A. Albrecht and P. J. Steinhardt, *Phys. Rev. Lett.* 48, 1220 (1982).
- [2] H. Murayama, H. Suzuki, T. Yanagida, and J. Yokoyama, *Phys. Rev. Lett.* 70, 1912 (1993); H. Murayama, H. Suzuki, T. Yanagida, and J. Yokoyama, *Phys. Rev. D* 50, 2356 (1994).
- [3] J. Ellis, M. Raidal and T. Yanagida, arXiv: hep-ph/0303242.
- [4] Y. Fukuda et al. [Super-Kamiokande Collaboration], *Phys. Rev. Lett.* 81 (1998) 1562; Q. R. Ahmad et al. [SNO Collaboration], *Phys. Rev. Lett.* 89 (2002) 011301, arXiv: nucl-ex/0204008; K. Eguchi et al. [KamLAND Collaboration], *Phys. Rev. Lett.* 90 (2003) 021802, arXiv: hep-ex/0212021.
- [5] M. Gell-Mann, P. Ramond and R. Slansky, *Proceedings of the Supergravity Stony Brook Workshop, New York, 1979*, eds. P. Van Nieuwenhuizen and D. Freedman (North-Holland, Amsterdam); T. Yanagida, *Proceedings of the Workshop on Unified Theories and Baryon Number in the Universe, Tsukuba, Japan 1979* (eds. A. Sawada and A. Sugamoto, KEK Report No. 79-18, Tsukuba); R. N. Mohapatra and G. Senjanovic, *Phys. Rev. Lett.* 44, 912 (1980); S. L. Glashow, *Caracese lectures*, (1979).
- [6] M. Fukugita and T. Yanagida, *Phys. Lett. B* 174 (1986) 45; P. Langacker, R. D. Peccei and T. Yanagida, *Mod. Phys. Lett. A* 1, (1986) 541; R. N. Mohapatra and X. Zhang, *Phys. Rev. D* 46, (1992) 5331; H. Murayama and T. Yanagida, *Phys. Lett. B* 322 (1994) 349 arXiv: hep-ph/9310297; K. Hamaguchi, H. Murayama and T. Yanagida, *Phys. Rev. D* 65 (2002) 043512

- arXiv:hep-ph/0109030; T. Moroi and H. Murayama, Phys. Lett. B 553 (2003) 126 arXiv:hep-ph/0211019.
- [7] C. L. Bennett et al., astro-ph/0302207.
- [8] G. Hinshaw et al., astro-ph/0302217.
- [9] C. L. Bennett et al., Astrophys. J. 464, L1 (1996).
- [10] H. V. Peiris et al., astro-ph/0302225.
- [11] W. J. Percival et al., Mon. Not. Roy. Astr. Soc. 327, 1297 (2001).
- [12] P. Mukherjee and Y. Wang, astro-ph/0303211.
- [13] S. L. Bridle, A. M. Lewis, J. Weller, and G. Efstathiou, astro-ph/0302306.
- [14] Y. Wang, D. N. Spergel, and M. A. Strauss, Astrophys. J. 510, 20 (1999); Y. Wang and G. Matthews, Astrophys. J. 573, 1 (2002); P. Mukherjee and Y. Wang, astro-ph/0301058; P. Mukherjee and Y. Wang, astro-ph/0301562.
- [15] D. N. Spergel et al., astro-ph/0302209.
- [16] J. M. Cline, P. Crotty and J. Lesgourgues, astro-ph/0304558; G. Efstathiou, astro-ph/0306431; A. d. Oliveira-Costa, M. Tegmark, M. Zaldarriaga and A. Hamilton, astro-ph/0307282; A. Niarhou, A. H. Jaffe and L. Pogosian, astro-ph/0308461.
- [17] Y.-P. Jing and L.-Z. Fang, Phys. Rev. Lett. 73, 1882 (1994); J. Yokoyama, Phys. Rev. D 59, 107303 (1999); S. DeDeo, R. R. Caldwell and P. J. Steinhardt, Phys. Rev. D 67, 103509 (2003); J. Uzan, A. Riazuelo, R. Lehoucq and J. Weeks, astro-ph/0303580; G. Efstathiou, Mon. Not. Roy. Astr. Soc. 343, L95 (2003); C. R. Contaldi, M. Peloso, L. Kofman, and A. Linde, JCAP 0307, 002 (2003); E. Gaztanaga, J. Wagg, T. Multamaki, A. Montana and D. H. Hughes, astro-ph/0304178; M. Kawasaki and F. Takahashi, hep-ph/0305319; M. Bastero-Gil et al., in Ref. [21]; A. Lasenby and C. Doran, astro-ph/0307311; S. Tsujikawa, R. Maartens and R. Brandenberger, astro-ph/0308169; T. Moroi and T. Takahashi, astro-ph/0308208; Q. Huang and M. Li, astro-ph/0308458.
- [18] B. Feng and X. Zhang, Phys. Lett. B 570, 145 (2003)
- [19] B. Feng, M. Li, R.-J. Zhang, and X. Zhang, astro-ph/0302479.
- [20] X. Wang et al., astro-ph/0209242.
- [21] J. E. Lidsey and R. Tavakol, astro-ph/0304113; M. Kawasaki, M. Yamaguchi and J. Yokoyama, Phys. Rev. D 68, 023508 (2003); Q. G. Huang and M. Li, JHEP 0306, 014 (2003); D. J. Chung, G. Shiu and M. Trodden, astro-ph/0305193; K.-I. Izawa, hep-ph/0305286; M. Bastero-Gil, K.

- Freese and L. Mersini-Houghton, hep-ph/0306289; M. Yamaguchi and J. Yokoyama, hep-ph/0307373.
- [22] V. Barger, H. Lee, and D. Marfatia, Phys.Lett.B 565, 33 (2003); W. H. Kinney, E. W. Kolb, A. Melchiorri and A. Riotto, hep-ph/0305130; S. M. Leach and A. R. Liddle, astro-ph/0306305.
- [23] D. Polarski and A. A. Starobinsky, Nucl.Phys.B 385, 623 (1992); D. Polarski, Phys.Rev.D 49, 6319 (1994); D. Polarski and A. A. Starobinsky, Phys.Lett.B 356, 196 (1995); J. Lesgourgues and D. Polarski, Phys.Rev.D 56, 6425 (1997).
- [24] M. H. Keskden, M. Kamionkowski and A. Cooray, astro-ph/0306597.
- [25] M. Kamionkowski, in private communications.
- [26] J. M. Diego, P. M. Mazzotta and J. Silk, astro-ph/0309181; O. Dore, G. P. Holder and A. Loeb, astro-ph/0309281; P. G. Castro, M. Douspis and P. G. Ferreira, astro-ph/0309320.
- [27] J. R. Ellis, J. E. Kin and D. V. Nanopoulos, Phys. Lett. B 145 (1984) 181; J. R. Ellis, D. V. Nanopoulos and S. Sarkar, Nucl. Phys. B 259 (1985) 175; J. R. Ellis, D. V. Nanopoulos, K. A. Olive and S. J. Rey, Astropart. Phys. 4 (1996) 371; M. Kawasaki and T. Mori, Prog. Theor. Phys. 93 (1995) 879; T. Mori, Ph.D. thesis, arXiv:hep-ph/9503210; M. Bolz, A. Brandenburg and W. Buchmuller, Nucl. Phys. B 606 (2001) 518; R. Cyburt, J. R. Ellis, B. D. Fields and K. A. Olive, astro-ph/0211258.
- [28] H. V. Klapdor-Kleingrothaus et al., Mod. Phys. Lett. A 16, 2409 (2002).
- [29] C. Gordon, D. Wands, B. A. Bassett, and R. Maartens, Phys. Rev. D 63, 023506 (2001).
- [30] S. M. Leach and A. R. Liddle, Phys. Rev. D 63, 043508 (2001); S. M. Leach, M. Sasaki, D. Wands and A. R. Liddle, Phys. Rev. D 64, 023512 (2001).
- [31] D. H. Huang, W. B. Lin and X. M. Zhang Phys.Rev.D 62, 087302 (2000).
- [32] B. Feng, X. Gong and X. Wang, astro-ph/0301111.
- [33] D. H. Lyth and A. Riotto, Phys.Rept. 314, 1 (1999).
- [34] L. Verde et al., arXiv: astro-ph/0302218.
- [35] A. R. Liddle and S. M. Leach, arXiv: astro-ph/0305263.
- [36] Z. Maki, M. Nakagawa, and S. Sakata, Prog. Theor. Phys. 28, 870 (1962).
- [37] J. A. Casas and A. Ibarra, Nucl. Phys. B 618, 171 (2001).
- [38] K. Hamaguchi, H. Murayama, T. Yanagida, Phys. Rev. D 65, 043512 (2002), arXiv: hep-ph/0109030.
- [39] W. Buchmuller, P. Di Bari and M. Plumacher, Nucl. Phys. B 643, 367 (2002).

- [40] M .L.B rooks et al, M E G A C ollaboration, Phys. Rev. Lett. 83 1521 (1999); S. A h m e d et al, C L E O C ollaboration, Phys. Rev. D 61 071101 (2000); U .B ellgardt et al, Nucl. Phys. B 229 1 (1988).
- [41] S. A ntusch, J. K ersten, M .L indner, M .R atz, arX iv: hep-ph/0305273.
- [42] X .J. B i, Y .P. K uang and Y .H .A n, arX iv: hep-ph/0211142.
- [43] U .S eljak and M .Z aldarriaga, A strophys. J. 469, 437 (1996).
- [44] <http://cmbfast.org/> .